Analysis of Reinforced Concrete Beams with Corrosion Damaged Stirrups for Shear Capacity

Christopher Higgins[1], William C. Farrow III[2], and O. Tugrul Turan[3]

[1] *Associate Prof.,* [3] *Graduate Research Asst., School of Civil and Constr. Eng., Oregon State University, Corvallis, OR 97331*

[2] *Structural Engineer, Gannett Fleming Engineers & Architects PC, New York City, NY 10001*

Corrosion of embedded carbon steel is a leading factor in deterioration of aging conventional reinforced concrete structures. Methods to accurately predict remaining capacity of corrosion damaged elements, especially shear capacity, are lacking. In this paper, ACI-AASHTO approach, Strut and Tie Method, Modified Compression Field Theory, and Response 2000 were used to predict the shear strength of corrosion damaged and undamaged test beams. The methods were modified to account for the corrosion induced damage to both the concrete section and stirrups. Each of the methods considered, with the proposed modifications, reasonably estimated the remaining shear capacity of large-size laboratory specimens subjected to accelerated corrosion of embedded stirrups.

Keywords: Corrosion; Deterioration; Girders; Reinforced concrete; Shear strength.

1. Introduction

Concrete generally provides excellent corrosion protection of embedded reinforcing steel. Corrosion of rebar, however, can occur for many reasons including inadequate concrete quality, improper design or detailing of the structure for the service environment, or because the environmental conditions are more aggressive or change during the anticipated service life of the structure (ACI Committee 222, 1996). Corrosion of embedded carbon steel reinforcement is a leading factor in the deterioration of aging conventional reinforced

concrete (CRC) bridges or other structures exposed to marine coastal environments. In 1998, there were approximately 235,000 CRC bridges in service in the United States. Of these, over 21,000 were rated as structurally deficient (Koch *et al.* 2002), many attributed to chloride-induced corrosion damage (Yunovich and Thompson 2003). Due to the large numbers of structurally deficient CRC bridges and the scarcity of resources for repair, rehabilitation, or replacement, many remain in service, even as they are subject to increased volume and weight of truck traffic. However, methods to accurately predict remaining capacity of corrosion damaged elements are lacking. Of particular concern may be the shear capacity of vintage CRC bridge girders and bents. Design practice prior to 1961 (AASHTO 1956) relied on the concrete to carry a larger proportion of the shear force than would be permitted by modern standards and thus these vintage elements may be considered lightly reinforced for shear. As a result, corrosion of stirrups may significantly impact the capacity of these elements.

Previous research related to corrosion effects on CRC element performance has focused in three main areas: flexural behavior of members, bond-slip behavior of rebar, and mechanical properties of corroded rebar. The behavior of corrosion damaged CRC elements tested in flexure indicated that as the reinforcing steel corrodes, load capacity and ductility are decreased (Al-Sulaimani *et al.* 1990, Almusallam *et al.* 1996, Cabrera 1996). Bond-slip behavior of corroded rebar samples indicates a loss of bond with increasing section-loss (Al-Sulaimani *et al.* 1990, Cabrera 1996, Amleh and Mirza 1999, Stanish *et al.* 1999). Tensile strength of corroded rebar has been shown to be little affected, but the overall ductility can be significantly reduced (Almusallam 2001, Palsson and Mirza 2002). Information on shear behavior of corrosion damaged beams is limited and analysis methods to predict the remaining strength of corrosion damaged CRC elements are lacking.

An experimental study of CRC beams with corrosion of shear stirrups was recently completed (Higgins and Farrow III 2006). Three different cross-sectional shapes were investigated: rectangular (R), inverted-T (IT), and T cross-sections. Specimens were subjected to accelerated corrosion of the embedded stirrups and then tested to failure under four-point bending. Yield strength of the flexural tension, flexural compression, and transverse steel was 72, 70, and 64 ksi (496, 482 and 441 MPa), respectively. Flexural steel was epoxy coated and adequately anchored with hooks to preclude anchorage failure. Physical dimensions of the beam specimens included a stem width of 10 in. (254 mm), an overall height of 24 in. (610 mm), an effective depth of 20.5 in. (521 mm) with a flexural reinforcement ratio (ρ) of 1.9% for rectangular and inverted-T cross-sections while an effective depth of 21.5 in (546 mm) with flexural reinforcement ratio of 1.8% for T cross-sections. Concrete cover was 1.5 in. (38 mm) for all specimens. The overall specimen length was 10 ft (3m) with 8 ft (2.4m) distance between centerline of supports. The shear span to effective depth ratio was equal to 2.05 for rectangular and T cross-sections while 1.95 for inverted-T cross-sections Stirrup spacing varied from 8 in. (203 mm) to 12 in. (305 mm) and four corrosion damage states were considered: no corrosion damage state A (control specimen), light damage state B with target average cross-sectional area loss of 12%, moderate damage state C with target average cross-sectional area loss of 20%, and severe damage state D corresponding to target average cross-sectional area loss of 40%. Localized cross-sectional area loss was observed to be much larger than the average cross-section for some of the specimens. Test specimens, their corresponding corrosion damage states, and key test results are summarized in Table 1. Actual stirrup areas for stirrups crossing the diagonal crack at failure are shown in Table 2. Average area was determined using the Gravimetric method and local minimum areas were determined using a contour gage (Farrow III 2003).

Specimens showed diminished strength and deformation capacity as the corrosion level increased. Locations and sequencing of damage to the stirrups could combine to produce particularly nonductile response and reduced strength. Additional details related to the accelerated corrosion and the resulting corrosion products which are not within the scope of this study can be found in Higgins *et al.* (2003).

2. Analysis of Corrosion Damaged Beams for Shear

Four different analysis methods were used to predict strength of corrosion damaged beam specimens. These include: traditional ACI approach (ACI Committee 318 2002, AASHTO 1996), Strut-and-Tie Method (STM) (ACI Committee 318 2002), Modified Compression Field Theory (MCFT) (AASHTO 2002), and Response 2000 (R2K) (Bentz 2000). Corrosion effects were incorporated in these methods by including concrete damage due to spalling and reduced stirrup area. Rebar section-loss was quantified using both average area along the bars as well as local minimum stirrup area. Predicted shear capacities were compared with experimental values.

2.1. *Conventional ACI-AASHTO Standard Specification Approach*

The traditional method for computing the shear strength of CRC elements consists of the superposition of the concrete and stirrup contributions to shear resistance (ACI Committee 318 2002, AASHTO 1996):

$$V_n = V_c + V_s \tag{1}$$

$$V_c = 2\sqrt{f'_c}\, b_w d \tag{2}$$

$$V_s = \frac{A_v f_{yt} d}{s} \tag{3}$$

where V_n is the nominal shear resistance (lb), V_c is the shear resistance of the concrete (lb), V_s is the shear resistance of the transverse steel (lb), f'_c is the compressive strength of the

concrete (psi), A_v is the area of the transverse steel (in^2), f_{yt} is the yield strength of the transverse steel (psi), d is the effective depth (in), b_w is the beam width (in), and s is the spacing of the transverse steel (in).

As members become deep (the shear span-to depth ratio decreases below about 2.5), the average shear stress at failure becomes progressively larger than in slender beams and it is easier for the shear to be transmitted directly to the support by a compression strut (ASCE-ACI Committee 445, 1999). Therefore, the ACI-AASHTO Standard Specification equations tend to underestimate concrete contributions to shear strength when the shear-span to depth ratio is less than 2.5. For the beams studied, the shear-span to depth ratio was approximately 2. Applying the conventional approach to estimate the concrete contribution to shear (Eq. 2) resulted in significant under-prediction of capacity for the undamaged specimens, on average by a factor of 1.53. Using experimentally measured shear strength and subtracting the stirrup contribution, a concrete shear stress coefficient was determined assuming the shear strength is related to the square root of the compressive strength, as in Eq. 2. It was found that a shear stress coefficient of 5 provided better prediction of the strength for the specimens, in place of the specified coefficient of 2:

$$V_{c(a/d=2)} = 5\sqrt{f'_c}\, b_w d \tag{4}$$

This is also observed in the literature for beams with shear-span to depth ratio values near 2, where the concrete shear stress multiplier was also found to be approximately 5 (Fereig and Smith 1977). Subsequent development of the proposed corrosion-damaged models for strength prediction was made using a concrete shear stress multiplier of 5, and provided more reasonable strength predictions for the undamaged beams.

Prediction of the shear capacity of corrosion damaged CRC sections requires modeling damage to the concrete from cracking and spalling as well as the section-loss and debonding of transverse steel. Methods were developed to treat these aspects of corrosion damage and results were compared with experimental findings.

Section-loss of the transverse steel from corrosion was directly quantified through measurement using two methods: average areas over the lengths of stirrups and local minimum areas of stirrups within a span length equal to the depth of the section. Example stirrup corrosion damage is illustrated in Fig. 1 for 10RD. Each of the legs was measured to quantify the average remaining rebar area over the length of the leg. The number of stirrups, n, crossing a potential diagonal crack oriented at an angle of 45^{o} is:

$$n=\frac{d}{s} \tag{5}$$

where s is the stirrup spacing and d is the beam depth. The average area ($\bar{A}_{v_i}$) for each stirrup was determined by summing the average area measurements for each leg:

$$\bar{A}_{v_i}=\bar{A}_{leg_1}+\bar{A}_{leg_2} \tag{6}$$

The average stirrup area within the region is determined by computing an equivalent stirrup area to be applied at the same spacing as that of the undamaged stirrups:

$$\bar{A}_v=\frac{\sum_{i=1}^{n}\bar{A}_{v_i}}{n} \tag{7}$$

This approach provided reasonable results for remaining capacity, as will be shown, but alternatively the analyst may wish to treat the beam as having a wider spacing of stirrups in combination with the equivalent average or minimum areas when one or more sequential stirrups are completely corroded.

To estimate local minimum area, the number of stirrups within the beam length for an assumed 45^o diagonal crack are computed by Eq. 5 and the minimum area for each stirrup within this region is determined. However, corrosion has been shown to decrease ductility of reinforcing steel (Almusallam 2001) and thus for cases where two legs of the same stirrup exhibit significantly different degrees of corrosion, the reduced ductility of one leg may limit the ability to achieve the combined strength of both legs. Previous tests on corroded rebar have shown that samples with up to 75% section loss provided sufficient ductility to achieve yield for Grade 60 uncorroded bar (Almusallam 2001). It is recommended that if one leg exhibits 75% more section loss than the other, the area of both legs be set to that of the smallest area. Further, it is assumed that if a stirrup has undergone complete section-loss of one leg, the stirrup would not be capable of effectively restraining a diagonal crack due to loss of bond around the legs. Thus, the area for both legs is set equal to zero. The smallest area for each stirrup ($\dot{A}_{v_i}$) is determined by summing the local minimum area measurements for each leg:

$$\dot{A}_{v_i} = \dot{A}_{leg_1} + \dot{A}_{leg_2} \quad ; \quad \text{if } \dot{A}_{leg_i} = 0 \text{ then } \dot{A}_{v_i} = 0 \tag{8}$$

The minimum stirrup area within the region is determined by computing an equivalent stirrup area to be applied at the same spacing as that of the undamaged stirrups:

$$\dot{A}_v = \frac{\sum_{i=1}^{n} \dot{A}_{v_i}}{n} \tag{9}$$

Average stirrup areas were found using the Gravimetric method, which required removal of the stirrup from the member. This is not possible in practice, and thus determining the average remaining area of the stirrups requires judgment of the inspector to determine where to make measurements and how many measurements are required. The cross-sections of highly-corroded rebar were observed to be quite random, however, rebar samples removed

from test specimens tended to be semi-circular on the surface in contact with the concrete core region. Thus, it is possible to estimate the area even if only half of the cross-section is available for measurement. On highly corroded rebar, there is often space behind the bar (due to area loss to corrosion) to measure the width in the transverse dimension. Measurements can be made using either digital calipers or a contour gage. A contour gage was able to capture the outward facing random rebar perimeter and the back half may then estimated as semi-circular. It is recommended at least three measurements be taken on a stirrup leg to get an average area and one of these should be at the location that exhibits the largest section loss. It was always conservative to take a single measurement of the minimum area on a stirrup leg and use this value in the previous calculations for determining the average area.

Once the equivalent corrosion-damaged stirrup area is determined, the steel contribution to shear resistance is computed by Eq. 3. The concrete damage from corrosion must then be estimated. This was done using empirical evidence and theoretical computation from observed cover damage due to spalling. Based on observed spall damage to the concrete cover from expansion of corrosion products, the concrete cross section was reduced. The amount of concrete damage depended primarily on stirrup spacing, cover distance, and degree of corrosion to underlying rebar. For larger spacing of the reinforcement and smaller cover, the cracks may tend to extend directly outward rather than reach out between the bars (Dagher and Kulendran 1992). Example spalling damage is illustrated in Fig. 2 and indicates that for widely spaced stirrups there is non-overlapping spall damage, but as the stirrup spacing becomes tighter, spall wedges will begin to interact and the entire cover area may spall. Based on observed spall patterns for experimental beams and field observed damage, the angle of discrete spalls was taken as approximately 20^{o}, originating at the intersection of the concrete core and the rebar cross-section. Using this angle for corrosion induced spalling

at stirrup locations and smearing the remaining area over the stirrup spacing, s, the effective concrete beam width available to resist shear may be estimated as:

$$b_{w_{eff}} = b_w - 2(c_v + \phi_v) + \frac{s}{5.5} \qquad \text{if } s \le 5.5(c_v + \phi_v) \qquad (10a)$$

$$b_{w_{eff}} = b_w - \frac{5.5}{s}(c_v + \phi_v)^2 \qquad \text{if } s > 5.5(c_v + \phi_v) \qquad (10b)$$

where b_w is the original undamaged beam width (in.), c_v is the concrete cover (in.), 1.5 in. (38 mm) for all specimens, ϕ_v is the stirrup diameter (in.), 0.5 in. (12.7 mm) for all specimens, and s is the stirrup spacing (in.). As the stirrup spacing becomes small, the effective concrete width approaches the core width. For the beams used in this study, the corrosion-damage induced effective widths were 7.5, 7.8, and 8.2 in. (189, 198, 208 mm) for the 8, 10, and 12 in. (203, 254 and 305 mm) stirrup spacings, respectively. Use of Eqs. 10a and 10b are for cases when the concrete cover is no longer effective, once significant corrosion induced cracks form on the concrete surface. Corrosion induced cracking was observed for experimental specimens at relatively small amounts of stirrup area section-loss (on average 2%). The damage progressed as additional corrosion occurred, with the cracks becoming larger and sounding indicated delaminations. When less stirrup section-loss has occurred, there may be some strength contribution attributed to partially damaged concrete cover.

Predicted shear capacity of the corrosion damaged beams using Eq. 10 for the effective concrete width and average stirrup areas applied at the original stirrup spacing (from Eqs. 5 to 7) are shown in Table 3 and Fig. 3. As seen in Table 3, the proposed equations provided a reasonably simple method to estimate shear capacity of corrosion damaged CRC beams in the absence of more sophisticated analyses (such as finite element analyses). The mean value for the ratio of experimental to predicted shear strength (V_{EXP}/V_n) was 1.13 with a coefficient of variation of 0.120. Using the minimum stirrup area calculated by Eqs. 8 and 9, in

combination with the predicted beam web widths of Eq. 10, the predicted shear strength tended to be less (in some cases significantly less) than the experimental results as seen in Table 3 and Fig. 3. For cases where the stirrups were completely corroded, the approach using the minimum area was overly conservative. A mean value for V_{EXP}/V_n = 1.28 with a coefficient of variation of 0.263 was observed by using the minimum stirrup area. Use of average values for stirrup area tended to provide better correlation with experimental results and indicate that some partial bonding of the stirrups may have permitted stirrups with locally significant section-loss (pits) to transfer stress between the rebar and concrete. This may have partially shielded the locally reduced stirrup area from strain concentrations, except when diagonal cracks formed adjacent to the pit location. In the field where concrete cover has completely spalled, it would be conservative to use the minimum stirrup area and to fully discount the contribution of any discontinuous stirrups.

2.2. STM Models for Corrosion Damaged Beams

The STM was also used to evaluate the shear strength of both corroded and uncorroded beams. A simplified strut-and-tie model was considered as shown in Fig. 4, to be consistent with likely practice implementation. The model consisted of four inclined struts, three horizontal struts, three tension ties, and eight nodes. The first tension tie (Tie 1) consisted of the flexural steel and the second two tension ties (Tie 2) represented the shear reinforcement. The amount of shear reinforcement included in Tie 2 was the area of stirrups crossing both inclined struts. The eight nodes consist of four CCT nodes (A and C), two CTT nodes (B), and two CCC nodes (D). Applying the ACI recommended β_n factors to the nodes resulted in failure at the CTT node (Node B) that was not observed in the tests. Setting the β_n factor for this node to unity caused failure in the two CCT nodes (Node A) at the bearing plates (which

were also not observed in the tests), therefore, β_n factors for these nodes were set to unity. Eventually, failure occurred in one of the two inclined struts or in Tie 2.

Nodes C and D were sized by setting the force couple from the flexural design equations to a maximum. This produced a 7 in. (178 mm) vertical height for specimens 8R, 10R, and 12R and 5 in. (127 mm) for specimen 10IT. The vertical height of Node D for specimen 10T was limited by the deck thickness, (4 in. [102 mm]) as the neutral axis was located in the deck.

Node A was determined by the length of the bearing plate (l_b) and the width of the tie (w_t), which was based on the distribution of flexural steel through the node. The bearing and loading plate lengths were 4 in. (102 mm) for all specimens, and the width of the tie region was 7 in. (178 mm) for 8R, 10R, 10T and 12R specimens, where two layers of flexural steel were present and 5 in. (127 mm) for inverted-T specimen where only a single layer of steel was used. The width of the struts, w_s, was determined as:

$$w_s = w_t \cos\theta + l_b \sin\theta \tag{11}$$

where θ (degrees) is the angle of the strut. The strut angles for the rectangular and T-beams were 39°, and 42° for the inverted-T beams. For beam series 8R, 10R, and 12R the struts were all prismatic with widths of 8 in. (203 mm) for Struts 1 and 2 and 7 in. (178 mm) for Struts 3 and 4. For the 10T series, Struts 1 and 2 had a width of 5.7 in. (145 mm), while Struts 3 and 4 were 4 in. (102 mm) wide. The width of Struts 1 and 2 was 6.4 in. (163 mm) and the width of Struts 3 and 4 was 5 in. (127 mm) for the 10IT series. For specimen 10T, the width of Strut 2 was 4 in. (102 mm) and a bottle strut was used for Strut 1, because the width of Node A was 8 in. (203 mm) and the width of Node C was 4 in (102 mm). As a consequence, the stress in the bottle strut was checked at each end. For specimen 10IT, the

width of Struts 1 and 2 were 6.2 in. (158 mm) and 5.7 in. (145mm), respectively. The size of Node B was selected to provide a prismatic strut for Strut 2.

The area of Tie 1 was 3.95 in^2 (2548 mm^2) for all specimens. Tie 2 represents the shear stirrups and the area varied depending on stirrup spacing. Tie 2 was 2.4 in^2 (1548 mm^2) (6 stirrups), 2.0 in^2 (1290 mm^2) (5 stirrups), and 1.6 in^2 (1032 mm^2) (4 stirrups) for beams with 8, 10, and 12 in. (203, 254, and 305 mm) stirrup spacing, respectively.

Predicted shear capacity for the damaged and undamaged specimens were tabulated in Table 3. As seen in this table, the selected STM reasonably estimated the shear capacity for all the undamaged beam configurations. The STM model had an average V_{EXP}/V_{STM} equal to 1.09 with a coefficient of variation of 0.035 for undamaged models.

Corrosion damage effects were incorporated in the STM by modifying two model attributes. Tension tie areas for the stirrups were reduced to reflect cross-sectional loss from corrosion. Strut widths were also reduced to reflect concrete cover damage due to spalling. Effective concrete widths were calculated by Eq. 11. Corrosion damage to the stirrups was considered in two ways, (1) the average section-loss along the length of the stirrups crossing the inclined struts (by Eqs. 5 to 7), and (2) the average of the local minimum stirrup areas crossing the inclined struts (Eqs. 5, 8 and 9).

Shear capacity of the corrosion damaged beams was fairly well predicted for the STM model using a reduced effective beam web width and average cross section-loss as shown in Table 3 and Fig. 5. The STM model with average stirrup area had a mean value of V_{EXP}/V_{STM} =1.16 with a coefficient of variation of 0.155. By comparison, the same model using reduced

vertical tension tie area according to the local minimum stirrup area tended to under estimate capacity more significantly and exhibited larger scatter as shown in Table 3 and shown in Fig. 5. The STM model using local minimum stirrup area had a V_{EXP}/V_{STM} mean value of 1.86 and the coefficient of variation was 0.656.

2.3 AASHTO LRFD Modified Compression Field Theory (MCFT)

Modified Compression Field Theory (MCFT) (Vecchio and Collins 1986) is the current shear design methodology prescribed by the AASHTO LRFD Bridge Design Specification (AASHTO 2002). MCFT takes into account residual concrete stresses in cracked concrete that permit the concrete section to resist higher shear forces. The model simplifies the complex shear behavior of a beam into a series of parallel diagonal cracks at an angle θ from horizontal, and assumes average stresses exist on the cross-section. MCFT may not predict shear capacity well for elements with an a/d ratio less than 2.5 (ASCE-ACI Committee 445 1999). The a/d ratio of the tested beams was 2.0. Therefore, while MCFT may not be best suited to predict the shear capacity of the specimens, however, it is used to demonstrate how corrosion damage can be incorporated into MCFT (results shown subsequently indicate that MCFT did predict shear capacity of the specimens reasonably well).

The shear capacity for a nonprestressed concrete beam is computed as in Eq. 1, with stirrup and concrete strength contributions dependent on diagonal crack angle and average strain on the section as:

$$V_S = \frac{A_V f_{yt} d_V \cot(\theta)}{s} \quad \text{for straight leg stirrups} \tag{12}$$

$$V_C = \beta \sqrt{f'_C}\, b_W d_V \tag{13}$$

where d_v is the distance between compression and tension resultants from moment equilibrium, and β is a factor related to θ, the crack angle, and ε_x, the average longitudinal strain in the section. When the cross-section has at least minimum stirrups, the average longitudinal strain can be determined as:

$$\varepsilon_x = \frac{\frac{M_u}{d_v} + 0.5\left(V_u \cot(\theta)\right)}{2E_s A_s} \leq 0.002 \qquad (14)$$

where M_u is the factored applied moment (lb-in), V_u is the factored applied shear (lb), A_s is the area of flexural steel that is adequately developed at the section (in^2), and E_s is the modulus of elasticity for the flexural steel (psi). If the section has less than minimum area of stirrups, Eq. 14 is multiplied by 2. Minimum stirrup area is defined as:

$$A_v = \left(\frac{1}{1000}\right)\sqrt{f'_c}\,\frac{b_w s}{f_{yt}} \quad \text{(units for } f_y \text{ and } f'_c \text{ are psi)} \qquad (15)$$

Values of β and θ are chosen from tables within the AASHTO specification and the capacity of the section is computed. Alternatively, Response 2000^{TM} (described below) may be used to generate AASHTO shear-moment interaction curves.

Corrosion damage was incorporated by reducing the beam effective width and considering two different types of damage to the stirrups: average area and minimum area. Predictions of shear capacity using the average stirrup section-loss are shown in Table 3 and Fig. 6. MCFT with average stirrup area provided a mean of V_{EXP}/V_{MCFT} = 1.38 and a coefficient of variation of 0.112. MCFT using local minimum area tended to underestimate shear capacity and had larger scatter as shown in Table 3 and Fig. 6. The average value of the V_{EXP}/V_{MCFT} = 1.75 with a coefficient of variation of 0.508.

2.4. Analysis by Response 2000^{TM}

The beam specimens were analyzed with a specialty computer program called Response 2000^{TM}. The program was developed at the University of Toronto (Bentz 2000) and uses a sectional analysis approach to assess the load-deformation response of cross-sections subject to bending moments, shear forces, and axial loads. Constitutive relationships between stresses and strains at a section are based on Modified Compression Field Theory. The program accommodates many different cross-sectional shapes, is easy to use, and is freely available at http://www.ecf.utoronto.ca/~bentz/r2k.htm. The program predicts the shear-moment failure surface for a specified cross-section, although the V-M response for high shear to moment ratios may not be as well predicted. Additionally, the program computes the AASHTO nominal V-M capacity curve based on MCFT for a specified cross-section.

Corrosion damage was incorporated by changing the effective beam web width and considering average area or minimum area due to section-loss of the stirrups. The results of R2K shear capacity prediction (using the sectional analysis feature) are shown in Table 3 and Fig. 7. Example shear force-midspan deflection response (using the member analysis feature of the program) for specimen 10RD is shown in Figs. 8. The prediction of shear capacity for corrosion damaged specimens could be significantly different, depending on the stirrup area chosen for the model. This difference is best illustrated for specimen 10RD shown in Fig. 8. Average and local maximum cross-sectional loss were 26% and 60%, respectively for this specimen and the impact on the model prediction is large. However, the response of the specimen prior to significant nonlinearity was similar for both approaches. The R2K analysis using average stirrup area provided a mean of $V_{EXP}/V_{R2K} = 1.17$ and a coefficient of variation of 0.114. The analysis using local minimum area tended to under-estimate shear capacity and

had larger scatter. Using the minimum stirrup area, resulted in a mean value for the V_{EXP}/V_{R2K} = 1.60 and a coefficient of variation of 0.625.

3. Discussion

The analysis methods with the proposed modifications to incorporate corrosion damage are summarized in Table 4 and normalized shear strength versus normalized stirrup quantity are plotted on Fig. 9 along with R2K, AASHTO-LRFD and ACI Method ($2\sqrt{f'_C}$) reference curves for 8RA. Reference curves were populated for more than minimum stirrup spacing specified in AASHTO-LRFD by changing the stirrup spacing. As seen here, each of the proposed analysis methods were able to conservatively predict the capacity of the specimens except for specimens 10RD and 10 ITD when using the average stirrup area. Use of average stirrup area for these analyses was possible due to partial bonding between the concrete and stirrups and sufficient ductility of pairs of corroded rebar legs which prevented locally reduced cross-sectional areas from controlling the strength of the specimens. In the field, cover spalling could be more substantial than that observed in the laboratory tests, and thus stirrups in service could fail at locally reduced cross-sections without transferring significant bond stresses between concrete and steel. Field inspection data should be used to guide the selection of the stirrup model.

As stated previously, specimens 10RD and 10 ITD were not predicted conservatively. These specimens exhibited the most significant corrosion damage with complete corrosion loss of some stirrups in the failure region. Additionally, sequential damage to adjacent stirrups and alignment of locally damaged regions along an eventual diagonal crack led to shear capacity less than that predicted. Therefore, caution should be exercised in the analysis of beams with severely corroded stirrups. For girders with sequential stirrups that are completely corroded,

analysts should consider using the average or local minimum rebar area at wider spacing than shown in the structural drawings to reflect the impact of sequential discontinuous stirrups. The lower shear capacity from this alternative or the proposed approach (using the specified spacing) should be used.

Methods for evaluation of existing structures, such as AASHTO LRFR (AASHTO 2003), generally incorporate a condition factor that represents strength reduction due to damage or deterioration. The condition factor is usually selected based on field inspection data that identify general member distress. Each of the corroded specimens was inspected per national bridge inspection (NBI) guidelines (Federal Highway Administration 1995). The corroded beams were given an Item #59 (superstructure) rating of 5 or 4, with 9 representing excellent condition and 0 representing failed condition. The assigned ratings would generally be recognized as corresponding to a LRFR condition factor of 0.85. The rating factors were essentially independent of the actual damage state (Higgins and Farrow III 2006). The experimentally observed strength reductions were compared with LRFR strength reduction factors and the predicted strength reductions based on the analysis methods outlined previously using average and minimum stirrup area. Results are shown in Table 5. It is observed that the LRFR condition factor does not consistently produce conservative results compared to the experimentally observed strength reductions. The proposed analysis methods provided more fidelity across the range of corrosion damaged specimens by better reflecting condition in the capacity model and provided more conservative results for the most deteriorated specimens. The key observation is that a prescriptive specification condition factor applied to the specified design strength cannot be used to represent the available strength of corroded RC girders for shear.

4. Conclusion

Although ACI-318 (ACI Committee 318 2002), AASHTO-LRFD (AASHTO 2002) and Canadian Highway Design Code (CSA International 2000) define a deep beam as a beam which has an a/d ratio less than 2 and recommend using strut and tie method for deep beam, since the specimens are at the transition zone between deep and slender beams and in order to demonstrate how corrosion damage to stirrups can be incorporated into current methods, several different analysis methods, more suitable for slender beams but still applicable to the current case, were used to predict the shear capacity of the damaged and undamaged test beams. The methods were modified to account for the corrosion induced damage to both the concrete section and stirrups. Both average and local minimum stirrup areas were considered in the analysis methods. Based on results of the analyses, the following conclusions are presented:

1. An analytical expression for concrete damage due to cover cracking and spalling was developed that depends on the amount of side cover and stirrup spacing.
2. Modeling stirrup corrosion damage using average rebar section-loss in combination with the concrete damage model provided better correlation with experimental results compared to use of minimum rebar section loss in combination with the concrete damage model.
3. Each of the methods considered could be used to reasonably estimate remaining shear capacity with the proposed modifications for corrosion damage.
4. Generic specification condition factors based on overall member condition may not adequately reflect the degree of strength reduction for significantly corroded specimens or may be overly conservative for lightly corroded specimens.
5. Average stirrup area provided the best prediction of the specimen strength, but for cases that exhibit more significant spalling or stirrup debonding, locally reduced cross-sectional

areas could control behavior. Field inspect data should be used to guide the approach used to model stirrup contributions.

6. Use of the minimum stirrup area provided conservative estimates of shear capacity for each of the methods, but was very conservative in some cases.
7. For girders with sequential stirrups that are completely corroded, analysts should consider using the average rebar area at wider spacing than shown in the structural drawings to reflect the impact of sequential discontinuous stirrups. The lower shear capacity from this alternative or the proposed approach should be used.
8. The program R2K provided not only capacity estimate, but also load-deformation response. While the displacements were not as well predicted as strength using this method, results provided an indication of the relative deformation capacity. Further, the program allowed quick computation of different input alternatives as well as the AASHTO LRFD MCFT shear-moment interaction capacity.

REFERENCES

AASHTO, "Standard Specification for Highway Bridges, Sixth Edition," AASHTO, Washington, D. C, 1953.

AASHTO, "Standard Specification for Highway Bridges, Sixteenth Edition," AASHTO, Washington, D. C., 1996.

AASHTO, "LRFD Bridge Design Specifications, Second Edition," AASHTO, Washington, D. C., 2002.

AASHTO, "Manual for Condition Evaluation and Load and Resistance Factor Rating (LRFR) of Highway Bridges," AASHTO, Washington, D. C., 2003.

ACI Committee 222, "Corrosion of Metals in Concrete," American Concrete Institute, Farmington Hills MI, 1996, pp., 30 pp.

ACI Committee 318, "Building Code Requirements for Structural Concrete," American Concrete Institute, Farmington Hills MI, 2002.

Almusallam, A. A., Al-Gahtani, A. S., Aziz, A. R., Dakhil, F. H., Rasheeduzzafar, "Effect of Reinforcement Corrosion on Flexural Behavior of Concrete Slabs," *Journal of Materials in Civil Engineering*, V. 8, No. 3, 1996, pp 123-127.

Almusallam, A. A., "Effect of Degree of Corrosion on the Properties of Reinforcing Steel Bars," *Construction and Building Materials*, V. 15, 2001, pp 361-368.

Al-Sulaimani, G. J., Kaleemullah, M., Basunbui, I. A., Rasheeduzzafar, "Influence of Corrosion and Cracking on Bond Behavior and Strength of Reinforced Concrete Members," *ACI Structural Journal*, V. 87, No. 2, 1990, pp 220-231.

Amleh, L., Mirza, S., "Corrosion Influence on Bond between Steel and Concrete," *ACI Structural Journal*, V. 96, No. 3, 1999, pp 415-423.

ASCE-ACI Committee 445, "Recent Approaches to Shear Design of Structural Concrete," *Journal of Structural Engineering*, V. 124, No. 12, 1999, pp 1375-1417.

Bentz, E, "Ph. D. Thesis: Sectional Analysis of Reinforced Concrete Members", University of Toronto, Toronto, Canada, 2000.

Cabrera, J. G., "Deterioration of Concrete Due to Reinforcement Steel Corrosion," *Cement and Concrete Composites*, V. 18, No. 1, 1996, pp 47-59.

CSA International, "Canadian Highway Bridge Design Code (CAN/CSA-S6-00)," Canadian Standards Association, Toronto, Ontario, Canada, 2000.

Dagher, H. J., Kulendran, "Finite Element Modeling of Corrosion Damage in Concrete Structures," *ACI Structural Journal*, V. 89, No. 6, 1992, pp 699-708.

Farrow, W. C. F. III, "MS. Thesis: Shear Capacity Assessment of Corrosion-Damaged Reinforced Concrete Beams," Oregon State University, 2003.

Federal Highway Administration, *Recording and Coding Guide for the Structure Inventory and Appraisal of the Nation's Bridges*, Report No. FHWA-PD-96-001, FHWA, Washington, DC., 1995.

Fereig, S. M., and Smith, K.N., "Indirect Loading on Beams with Short Shear Spans," *American Concrete Institute*, Journal Proceedings, V. 74, No.5, 1977, pp.220-222.

Higgins, C., Farrow, W. C., Potisuk, T., Miller, T. H., Yim, C. C., Cramer, S. D., Covino, Jr., B. S., Holcomb, G.R., Bullard, S. J. , Ziomek-Moroz, M., and Matthes, S. A., "Shear Capacity Assessment of Corrosion Damaged Reinforced Concrete Beams," Project SPR 326, Oregon Department of Transportation, 2003.

Higgins, C. and Farrow III, W. C., "Test of Reinforced Concrete Beams with Corrosion-Damage Stirrups," *ACI Structural Journal*, V.103, No.1, 2006, pp 133-141.

Koch, G. H., M. H. P. Brongers, N. G. Thompson, Y. P. Virmani, and J. H. Payer, *Corrosion Cost and Preventive Strategies in the United States*, Report no. FHWA-RD-01-156, Federal Highway Administration, U. S. Department of Transportation, Washington D.C., 2002, 773 pp.

Palsson, R., and M. S Mirza, "Mechanical Response of Corroded Steel Reinforcement of Abandoned Concrete Bridge," *ACI Structural Journal,* V. 99, No. 2, 2002, pp 157-162.

Stanish, K, Hooton, R. D., Pantazopoulou, S. J., "Corrosion Effects on Bond Strength in Reinforced Concrete," *ACI Structural Journal,* V. 96, No. 6, 1999, pp 915-921.

Vecchio, F. J., Collins, M. P., "The Modified Compression-Field Theory for Reinforced Concrete Elements Subjected to Shear", *Journal of The American Concrete Institute,* V. 83, No. 2, 1986, pp. 219-231.

Yunovich, M. and Thompson, N.G., "Corrosion of Highway Bridges: Economic Impact and Control Methodologies," *Concrete International,* V. 25, No. 1, 2003, pp 52-57.

TABLES AND FIGURES

List of Tables:

List of Figures:

Table 1 – Summary of experimental results

Beam Type	Stirrup Spacing cm (in)	d mm (in)	r -	f'c Mpa (psi)	Stirrup Fracture	Shear ($V_{EXP\ with\ self\text{-}weight}$) kN (kips)
8RA	20 (8)	521 (20.5)	0.019	29.3 (4250)	NO	612 (137.7)
8RD	20 (8)	521 (20.5)	0.019	29.3 (4250)	YES	485 (109.1)
10RA	25 (10)	521 (20.5)	0.019	33.4 (4850)	NO	597 (134.2)
10RB	25 (10)	521 (20.5)	0.019	33.4 (4850)	NO	522 (117.3)
10RC	25 (10)	521 (20.5)	0.019	33.4 (4850)	YES	482 (108.3)
10RD	25 (10)	521 (20.5)	0.019	33.4 (4850)	YES	419 (94.3)
10TA	25 (10)	521 (20.5)	0.019	36.5 (5300)	NO	650 (146.2)
10TC	25 (10)	521 (20.5)	0.019	36.5 (5300)	YES	484 (108.8)
10TD	25 (10)	521 (20.5)	0.019	36.5 (5300)	YES	606 (136.3)
10ITA	25 (10)	546 (21.5)	0.018	32.1 (4650)	NO	624 (140.3)
10ITC	25 (10)	546 (21.5)	0.018	32.1 (4650)	NO	592 (133.1)
10ITD	25 (10)	546 (21.5)	0.018	32.1 (4650)	YES	372 (83.6)
12RA	30 (12)	521 (20.5)	0.019	32.1 (4650)	NO	508 (114.2)
12RD	30 (12)	521 (20.5)	0.019	32.1 (4650)	YES	458 (102.9)

Table 2 – Amount of stirrup cross sectional area lost due to corrosion

Beam Type	Measured Area, mm^2 (in^2)			Stirrup Leg Section Loss %		
	Avg.*	Avg. of Min.**	Single Min.***	Avg	Avg. Min.	Single Min.
8RA	129.0 (0.20)	129.0 (0.20)	129.0 (0.20)	0.0	0.0	0.0
8RD	91.6 (0.14)	71.6 (0.11)	46.5 (0.07)	28.9	44.6	64.0
10RA	129.0 (0.20)	129.0 (0.20)	129.0 (0.20)	0.0	0.0	0.0
10RB	112.3 (0.17)	89.0 (0.14)	81.9 (0.13)	13.2	31.1	36.5
10RC	99.4 (0.15)	80.0 (0.12)	51.0 (0.08)	23.1	37.8	60.5
10RD	95.5 (0.15)	51.6 (0.08)	0.0 (0.00)	26.0	60.0	100.0
10TA	129.0 (0.20)	129.0 (0.20)	129.0 (0.20)	0.0	0.0	0.0
10TC	103.2 (0.16)	59.4 (0.09)	34.8 (0.05)	20.2	54.3	73.0
10TD	87.1 (0.14)	0.0 (0.00)	0.0 (0.00)	32.6	100.0	100.0
10ITA	129.0 (0.20)	129.0 (0.20)	129.0 (0.20)	0.0	0.0	0.0
10ITC	106.5 (0.17)	94.2 (0.15)	91.6 (0.14)	17.4	27.0	29.0
10ITD	82.6 (0.13)	58.1 (0.09)	36.1 (0.06)	35.9	55.1	72.0
12RA	129 (0.20)	129 (0.20)	129 (0.20)	0.0	0.0	0.0
12RD	85.8 (0.13)	39.4 (0.06)	0.0 (0.00)	33.8	69.4	100.0

(* = Stirrup leg area determined by averaging the average remaining areas of all stirrups in the test span, ** = stirrup leg area determined by averaging the localized minimum remaining areas of all stirrups in the test span, *** = Smallest remaining area for any single stirrup leg within the test span)

Table 3 – Predicted shear strength by ACI-AASHTO approach, STM, MCFT, and R2K with average and minimum stirrup areas and corrosion damaged concrete width.

Beam	$b_{w\ eff}$	ACI-AASHTO		STM		MCFT		R2K	
		$V_{n\ Avg.}$	$V_{n\ Min.}$	$V_{n\ Avg.}$	$V_{n\ Min.}$	$V_{n\ Avg.}$	$V_{n\ Min.}$	$V_{n\ Avg.}$	$V_{n\ Min.}$
	mm (in)	kN (kips)	kN (kips)	kN (kips)	kN (kips)	kN (kips)	kN (kips)	kN (kips)	kN (kips)
8RA	254 (10.0)	589 (132.4)	589 (132.4)	576 (129.6)	576 (129.6)	480 (107.9)	480 (107.9)	558 (125.5)	558 (125.5)
8RD	189 (7.5)	429 (96.4)	384 (86.2)	430 (96.6)	379 (85.1)	367 (82.5)	321 (72.2)	422 (94.8)	369 (82.9)
10RA	254 (10.0)	551 (123.9)	551 (123.9)	569 (128.0)	569 (128.0)	434 (97.5)	434 (97.5)	523 (117.7)	523 (117.7)
10RB	198 (7.8)	451 (101.3)	409 (91.9)	494 (111.1)	414 (93.0)	376 (84.5)	333 (74.9)	445 (100.1)	391 (88.0)
10RC	198 (7.8)	427 (96.1)	392 (88.2)	438 (98.5)	354 (79.6)	352 (79.2)	315 (70.9)	416 (93.6)	369 (82.9)
10RD	198 (7.8)	420 (94.5)	341 (76.7)	423 (95.0)	228 (51.2)	345 (77.6)	256 (57.6)	407 (91.5)	286 (64.4)
10TA	254 (10.0)	565 (127.1)	565 (127.1)	569 (128.0)	569 (128.0)	462 (103.8)	462 (103.8)	542 (121.8)	542 (121.8)
10TC	198 (7.8)	446 (100.2)	366 (82.3)	458 (102.9)	184 (41.3)	383 (86.1)	292 (65.6)	451 (101.4)	334 (75.1)
10TD	198 (7.8)	416 (93.6)	259 (58.2)	384 (86.3)	114 (25.6)	351 (78.9)	128 (28.7)	414 (93.0)	123 (27.6)
10ITA	254 (10.0)	571 (128.3)	571 (128.3)	569 (128.0)	569 (128.0)	452 (101.6)	452 (101.6)	538 (120.9)	538 (120.9)
10ITC	198 (7.8)	456 (102.6)	433 (97.4)	470 (105.7)	457 (102.7)	381 (85.6)	357 (80.2)	442 (99.4)	415 (93.3)
10ITD	198 (7.8)	411 (92.4)	365 (81.9)	365 (82.1)	175 (39.4)	333 (74.9)	281 (63.1)	384 (86.4)	297 (66.7)
12RA	254 (10.0)	494 (110.9)	494 (110.9)	455 (102.4)	455 (102.4)	386 (86.8)	386 (86.8)	454 (102.1)	454 (102.1)
12RD	207 (8.2)	374 (84.0)	304 (68.2)	302 (67.8)	134 (30.1)	296 (66.5)	213 (47.8)	336 (75.5)	214 (48.2)

Table 4 – Summary of the corrosion damaged specimens.

Beam	$V_{EXP}/V_{Predicted}$							
	ACI-AASHTO		STM		MCFT		R2K	
	Avg.	Min.	Avg.	Min.	Avg.	Min.	Avg.	Min.
8RD	1.13	1.27	1.13	1.28	1.32	1.51	1.15	1.32
10RB	1.16	1.28	1.06	1.26	1.39	1.57	1.17	1.33
10RC	1.13	1.23	1.10	1.36	1.37	1.53	1.16	1.31
10RD	1.00	1.23	0.99	1.84	1.22	1.64	1.03	1.46
10TC	1.09	1.32	1.06	2.64	1.26	1.66	1.07	1.45
10TD	1.46	2.34	1.58	5.32	1.73	4.75	1.47	4.94
10ITC	1.30	1.37	1.26	1.30	1.56	1.66	1.34	1.43
10ITD	0.90	1.02	1.02	2.12	1.12	1.33	0.97	1.25
12RD	1.23	1.51	1.52	3.42	1.55	2.15	1.36	2.13
Mean	1.15	1.40	1.19	2.28	1.39	1.98	1.19	1.85
COV	0.140	0.271	0.183	0.595	0.138	0.538	0.139	0.645

Table 5 – Strength reductions for experimental results, analysis methods, and LRFR condition factor.

Beam	Strength Reduction Coefficient									
	Experiment	ACI-AASHTO		STM		MCFT		R2K		LRFR
	-	Avg.	Min.	Avg.	Min.	Avg.	Min.	Avg.	Min.	-
8RA	1.00	1.00	1.00	1.00	1.00	1.00	1.00	1.00	1.00	1.00
8RD	0.79	0.73	0.65	0.75	0.66	0.77	0.67	0.76	0.66	0.85
10RA	1.00	1.00	1.00	1.00	1.00	1.00	1.00	1.00	1.00	1.00
10RB	0.87	0.82	0.74	0.87	0.73	0.87	0.77	0.85	0.75	0.85
10RC	0.81	0.78	0.71	0.77	0.62	0.81	0.73	0.80	0.70	0.85
10RD	0.70	0.76	0.62	0.74	0.40	0.80	0.59	0.78	0.55	0.85
10TA	1.00	1.00	1.00	1.00	1.00	1.00	1.00	1.00	1.00	1.00
10TC	0.74	0.79	0.65	0.80	0.32	0.83	0.63	0.83	0.62	0.85
10TD	0.93	0.74	0.46	0.67	0.20	0.76	0.28	0.76	0.23	0.85
10ITA	1.00	1.00	1.00	1.00	1.00	1.00	1.00	1.00	1.00	1.00
10ITC	0.95	0.80	0.76	0.83	0.80	0.84	0.79	0.82	0.77	0.85
10ITD	0.60	0.72	0.64	0.64	0.31	0.74	0.62	0.71	0.55	0.85
12RA	1.00	1.00	1.00	1.00	1.00	1.00	1.00	1.00	1.00	1.00
12RD	0.90	0.76	0.61	0.66	0.29	0.77	0.55	0.74	0.47	0.85

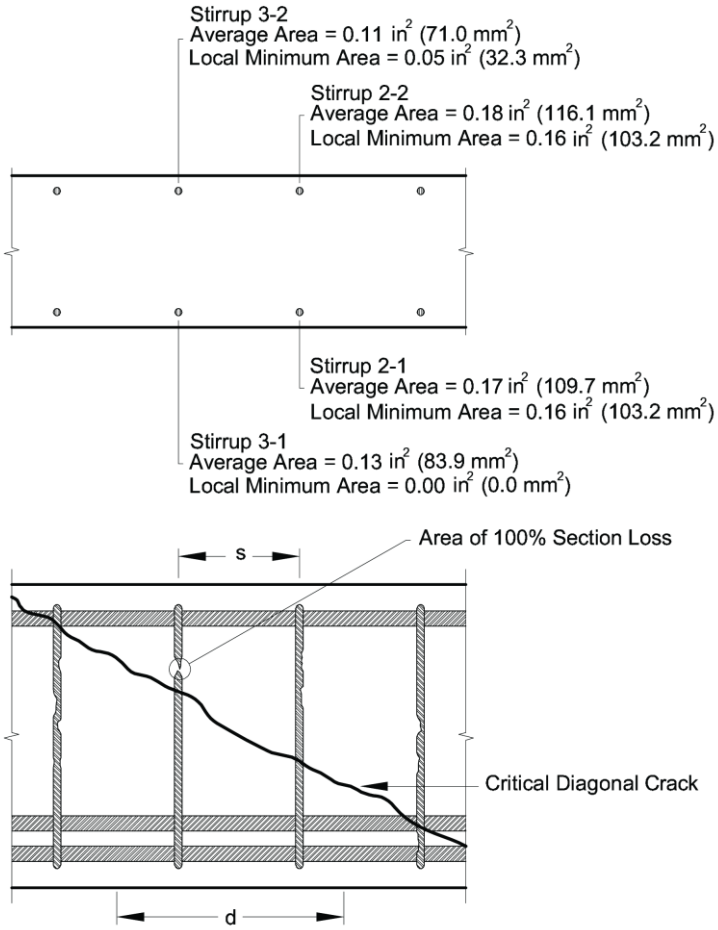

Fig. 1 – Average and local maximum section-loss of stirrups within a length of beam.

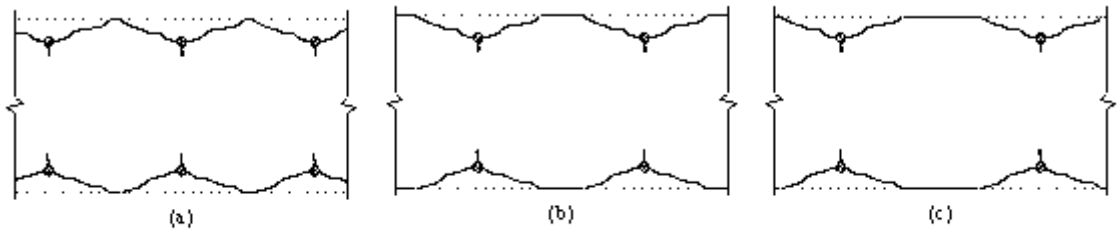

Fig. 2 – Plan view of concrete cracking in beam web due to corrosion for three different stirrup spacing; (a) 8-in (203 mm), (b) 10-in (254 mm), and (c) 12-in (305 mm).

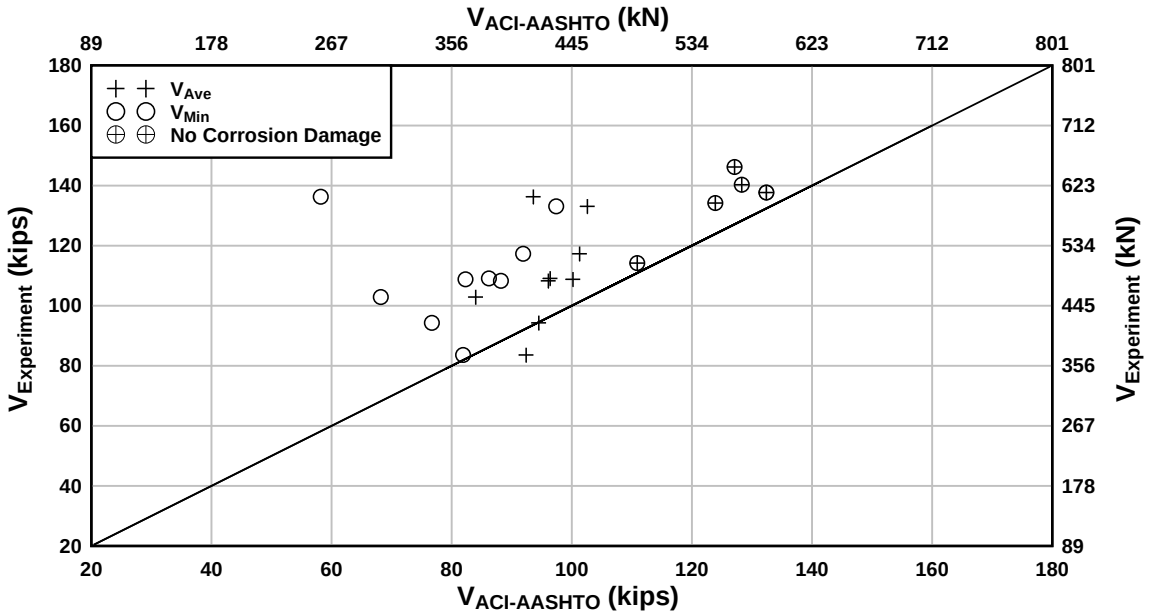

Fig. 3 – Ratio of experimental to predicted shear strengths for ACI-AASHTO approach including corrosion damage.

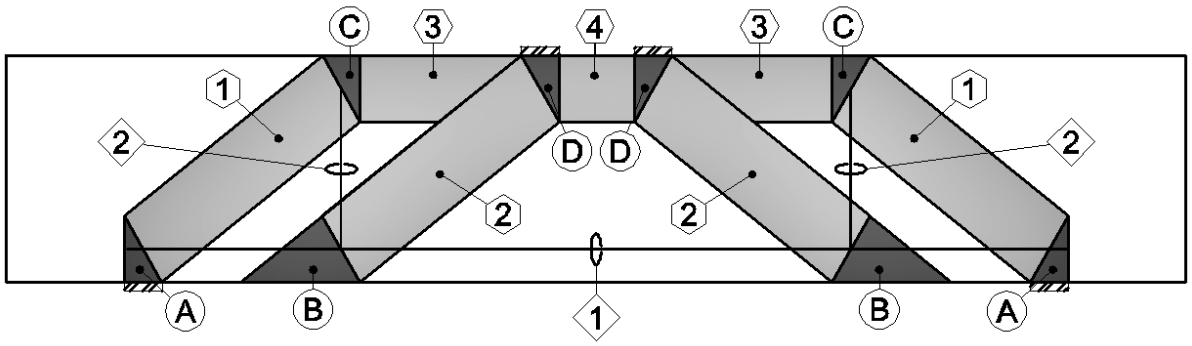

Fig. 4 – Strut-and-Tie model.

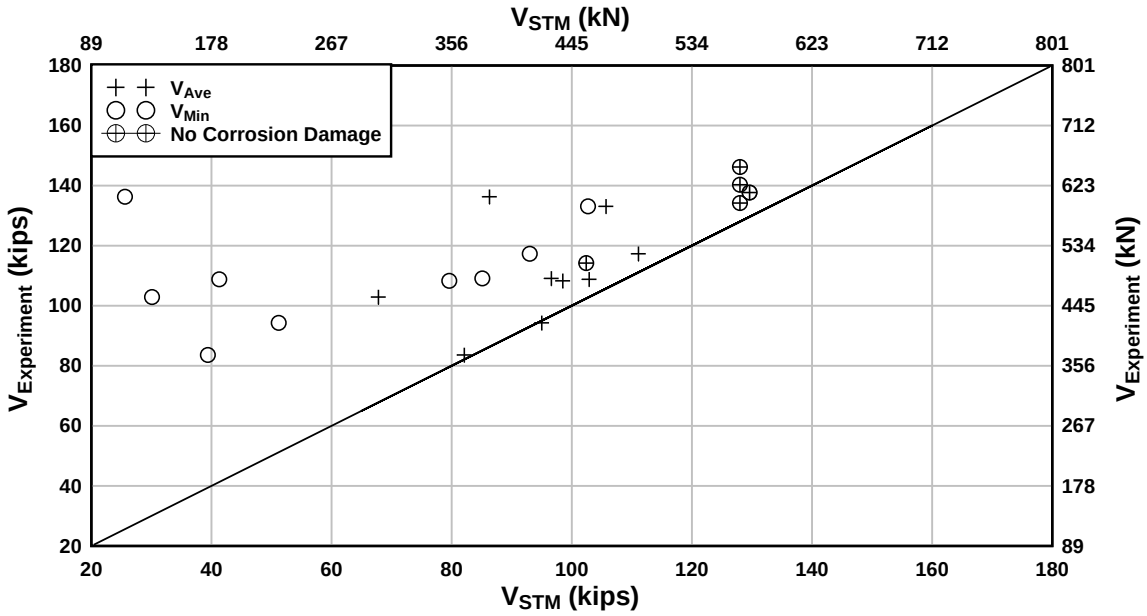

Fig. 5 – Experimental and analytical prediction of shear capacity from STM model

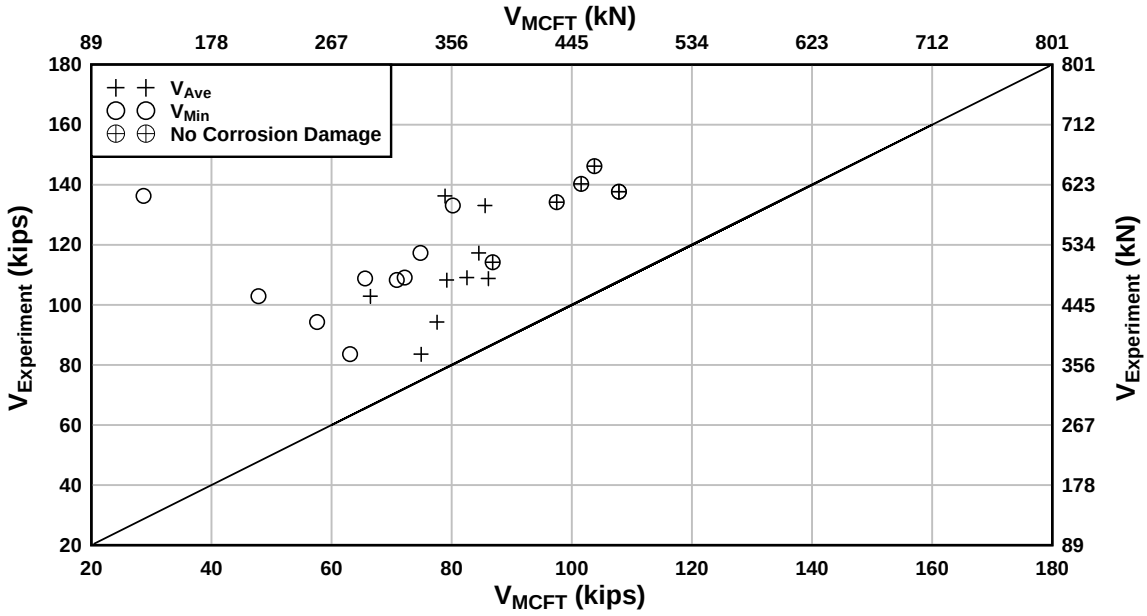

Fig. 6 – Experimental and analytical prediction of shear capacity from MCFT

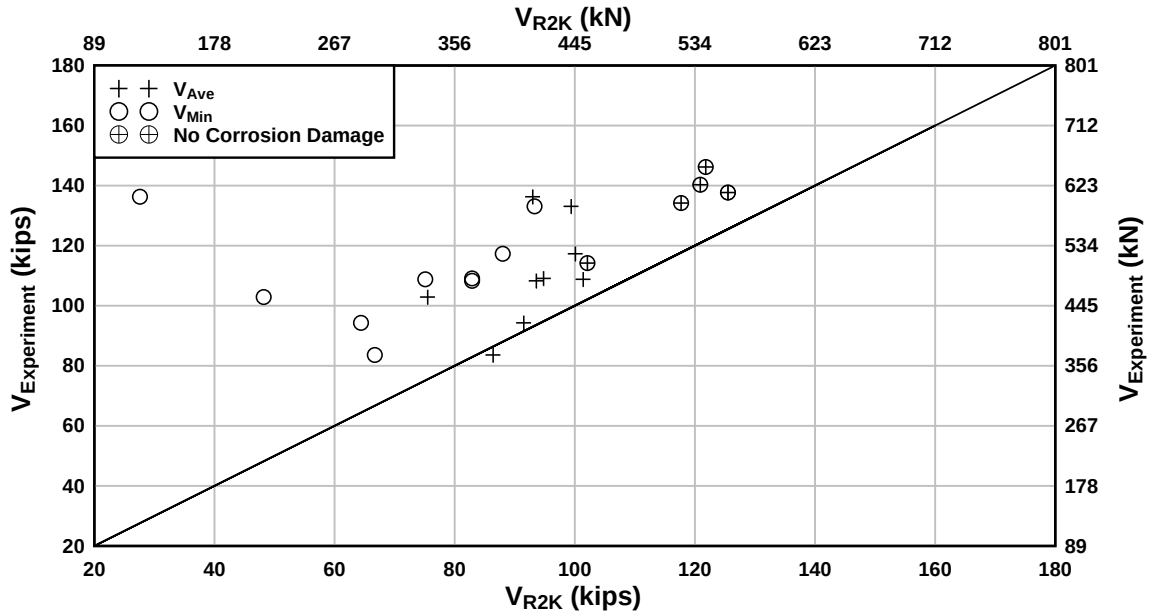

Fig. 7 – Experimental and analytical prediction of shear capacity from Response 2000.

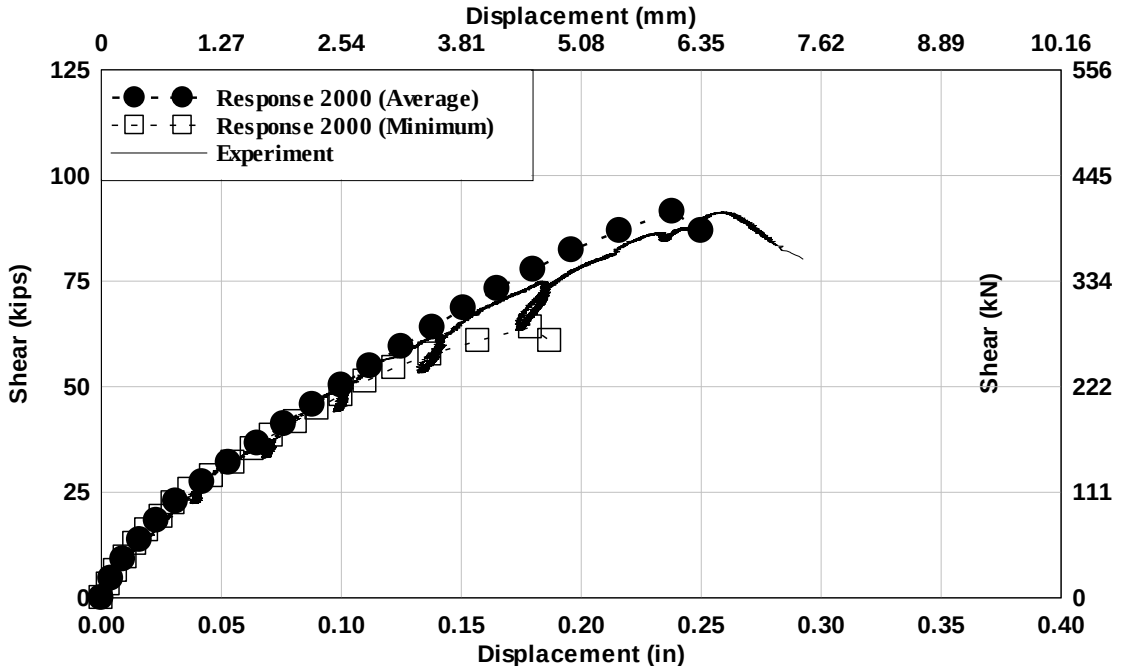

Fig. 8 – Experimental and analytical prediction of shear capacity from Response 2000, specimen 10RD.

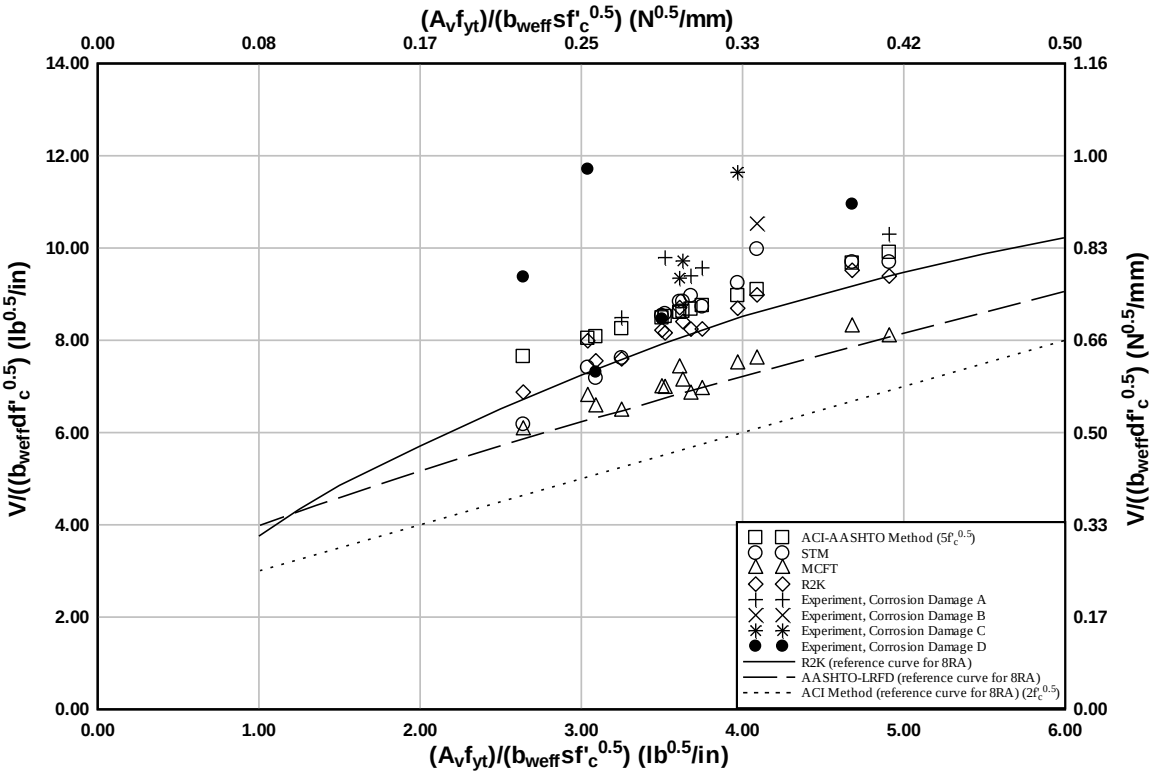

Fig. 9 – Normalized shear strength versus normalized stirrup quantity of all specimens.